Ring-Closing Olefin Metathesis on Ruthenium Carbene Complexes: Model DFT Study of Stereochemistry

Sergei F. Vyboishchikov[a, b] and Walter Thiel*[a]

Abstract: Ring-closing metathesis (RCM) is the key step in a recently reported synthesis of salicylihalamide and related model compounds. Experimentally, the stereochemistry of the resulting cycloolefin (*cis*/*trans*) depends strongly on the substituents that are present in the diene substrate. To gain insight into the factors that govern the observed stereochemistry, density functional theory (DFT) calculations have been carried out for a simplified dichloro(2-propylidene)(imidazole-2-ylidene)ruthenium catalyst **I**, as well as for the real catalyst **II** with two mesityl substituents on the imidazole ring. Four model substrates are considered, which are closely related to the systems studied experimentally, and in each case, two pathways A and B are possible since the RCM reaction can be initiated by coordination of either of the two diene double bonds to the metal center. The first metathesis yields a carbene intermediate, which can then undergo a second metathesis by ring closure, metallacycle formation, and metallacycle cleavage to give the final cycloolefin complex. According to the DFT calculations, the stereochemistry is always determined in the second metathesis reaction, but the rate-determining step may be different for different catalysts, substrates, and pathways. The ancillary N-heterocyclic carbene ligand lies in the Ru-Cl-Cl plane in the simplified catalyst **I**, but is perpendicular to it in the real catalyst **II**, and this affects the relative energies of the relevant intermediates and transition states. Likewise, the introduction of methyl substituents in the diene substrates influences these relative energies appreciably. Good agreement with the experimentally observed stereochemistry is only found when using the real catalyst **II** and the largest model substrates in the DFT calculations.

Keywords: alkenes · cyclization · density functional calculations · metathesis · reaction mechanisms

Introduction

Though discovered in the 1950s, olefin metathesis acquired importance as an efficient method for the formation of carbon–carbon double bonds only much later.[1–4] At present, it is used extensively in organic synthesis. The applications include ring-opening metathesis polymerization (ROMP), ring-closing metathesis (RCM), ring-opening metathesis (ROM), acyclic diene metathesis polymerization (ADMET), and cross-metathesis (CM). Ring-closing metathesis deserves special attention because it provides a powerful method for synthesizing large unsaturated rings from α,ω-diene precursors. In practice, broad usage of RCM was initially hampered by the nonselectivity of the early heterogeneous metathesis catalysts and their sensitivity toward functional groups, but more recently, a number of well-defined homogeneous organotransition–metal catalysts have been developed. Schrock's rhenium, molybdenum, and tungsten alkoxyimine or alkoxycarbene complexes are an important class of such catalysts.[5] They exhibit high activity, are quite tolerant to functional groups, and can be easily tuned to a particular substrate by appropriately chosen alkyl substituents. Their main drawback is high sensitivity to water and air. The ruthenium-based catalysts introduced by Grubbs et al.[4,6,7] with the general formula $[(PR_3)_2X_2Ru{=}CHR']$ (X = halide) exhibit high performance and superb tolerance against many common functional groups and are quite insensitive towards air and water. An even higher activity can be achieved if one of the trialkylphosphane ligands is replaced by an N-heterocyclic (Arduengo-type) carbene (NHC).[8–11] Another subgroup of ruthenium-based cat-

[a] Dr. S. F. Vyboishchikov, Prof. Dr. W. Thiel
Max-Planck-Institut für Kohlenforschung
Kaiser-Wilhelm-Platz 1, 45470 Mülheim/Ruhr (Germany)
Fax: (+49) 208-306-2996
E-mail: thiel@mpi-muelheim.mpg.de

[b] Dr. S. F. Vyboishchikov
Institut de Química Computacional
Campus de Montilivi, Universitat de Girona
17071 Girona, Catalonia (Spain)

Supporting information for this article is available on the WWW under http://www.chemeurj.org/ or from the author.

 DOI: 10.1002/chem.200400994

alysts are carbene complexes with chelating bis(phosphane) ligands and hence *cis* stereochemistry.[12]

According to the generally accepted Hérisson–Chauvin mechanism,[13] the actual metathesis occurs between a transition-metal carbene complex and an olefin moiety. In detail, it consists of series of formal [2+2] cycloadditions and cycloreversions, that is, olefin coordination to the transition-metal carbene complex to form a π complex, followed by migratory insertion of the olefin ligand into the metal–carbene bond to yield a metallacyclobutane, breaking of two different bonds in the metallacyclobutane to form another π complex, and dissociation to give the products (see Scheme 1). These general mechanistic features may vary depending on the particular catalyst chosen. Ruthenium–carbene catalysts were studied mechanistically both in solution[14–18] and in the gas phase.[19–23] There is substantial evidence[17–21] that the reaction favors the dissociative pathway, that is, the reactive catalytic species formed from pentacoordinate $[(PR_3)_2X_2Ru{=}CHR']$ or $[(PR_3)(NHC)X_2Ru{=}CHR']$ is actually the tetracoordinate 14-electron complex $[(PR_3)X_2Ru{=}CHR']$ or $[(NHC)X_2Ru{=}CHR']$, respectively. The subsequent steps in the catalytic cycle have not yet been characterized experimentally, and it has remained unclear, for example, whether the incoming olefin coordinates to the 14-electron intermediate in *cis* or *trans* position with respect to the ancillary ligand and whether the metallacyclobutane is actually an intermediate or merely a transition state.[18]

Such issues can be examined by means of quantum-chemical calculations. Until recently, theoretical calculations on olefin metathesis remained scarce. There were early computational studies on titanium-[24] and later on molybdenum-catalyzed[25–27] metathesis. Metathesis reactions on model ruthenium–carbene complexes $[(PH_3)_2Cl_2Ru{=}CH_2]$ were examined by using Car–Parrinello molecular dynamics,[28] but without addressing mechanistic details. Two extensive studies on Grubbs-type catalysts have been published recently,[29,30] which are complementary in essence. While our work[29] mostly concentrated on comparison of various possible reaction pathways, Cavallo[30] focused on substituent, ligand, and solvent effects. It was shown that the reaction takes place according to the dissociative mechanism with *trans* orientation of the incoming olefin,[29] because the other possibilities are impeded by a high barrier for initial olefin coordination. The ruthenacyclobutane was found to be a true intermediate, which is more stable than the olefin carbene complex for NHC-containing systems but less stable for phosphane systems.[29,30] Thus, the rate-determining step is either olefin insertion (for phosphane-containing catalysts) or the reverse reaction of ruthenacycle cleavage (for NHC-containing catalysts). The role of the solvent lies mainly in facilitating phosphane dissociation while not affecting olefin coordination.[30] In recent extensive computational work, Adlhart and Chen[31] showed that the reaction profile strongly depends on the olefin substrate as well as on ancillary ligands. Another computational study on a model system was presented by Bernardi et al.,[32] who considered three different pathways (one dissociative and two associative with or without "carbenoid" intermediates of the kind $[(PR_3)_2ClRu{-}CH_2Cl)]$. According to this work, the carbenoids may play a role in the associative mechanism by facilitating ruthenacycle formation. In another recent paper,[33] Cavallo and Costabile addressed the mechanism of enantioselectivity in asymmetric Ru-catalyzed RCM reactions with chiral NHC ligands, which induce enantioface selectivity through a chiral folding of NHC substituents.

The ring-closing metathesis of dienes consists of two successive metathesis reactions (Scheme 2). The only difference from usual cross-metathesis is ring closing in the fifth step, which in this case is an intramolecular process and will therefore have a barrier because of the distortions needed to coordinate the remaining C=C bond. In the intermolecular case, the coordination of a sterically unencumbered second olefin is normally barrier-free.

Our interest in the mechanism of ruthenium-catalyzed metathesis was prompted by surprising stereochemical observations made in the RCM step of the total synthesis of salicylihalamide.[34,35] This metabolite, isolated from the marine sponge *Haliclona*, attracted attention due to its pronounced antitumor activity. In recent years, several synthetic

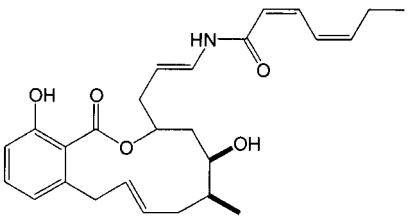

(–)-Salicylihalamide

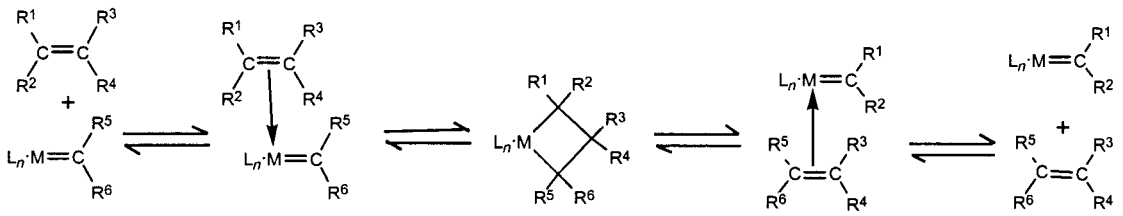

Scheme 1. Generalized Hérisson–Chauvin mechanism of olefin metathesis.

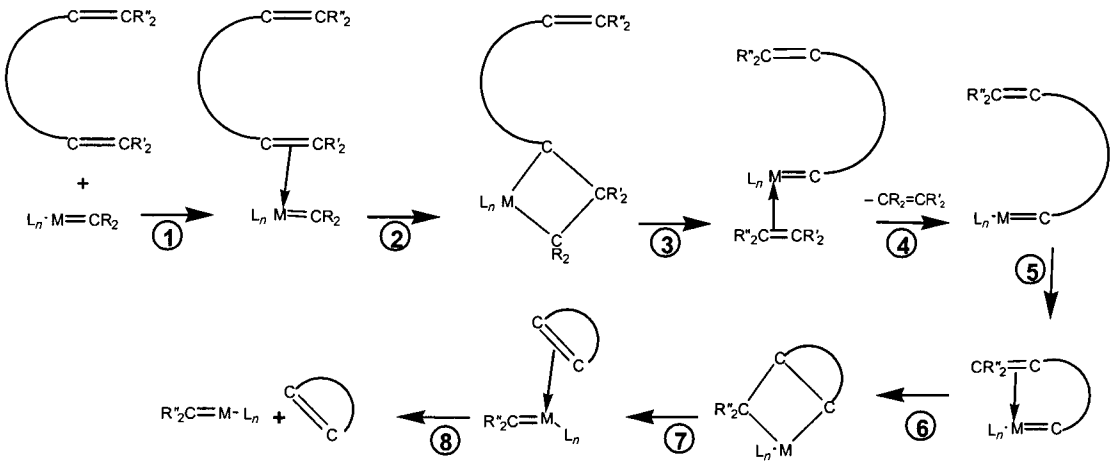

Scheme 2. Mechanism of ring-closing olefin metathesis.

routes to salicylihalamide were reported.[34–39] Though differing in many aspects, some of the stategies proposed[34–36,39] take advantage of ring-closing olefin metathesis with ruthenium catalysts to form a 12-membered ring that is essential to the salicylihalamide structure. Analogous cyclizations were performed[35] in model compounds (Scheme 3). Both in the model and the full salicylihalamide system, different stereochemistry with respect to the newly formed double bond was observed[35] depending on the substituents R and R^1. Cyclization of the model system yielded the *cis* product exclusively in the case R = H, whereas for R = *t*BuMe$_2$Si (TBS) the *cis*/*trans* ratio was 70/30. Similarly, for the full system, the *cis* product also prevailed for R = H, while R = TBS gave a *cis*/*trans* ratio of 60/40. However, inverted *cis*/*trans* ratios of 34/66 and 32/68 were observed for R = CH_3 and for R = CH_3OCH_2, respectively. The fact that these results are remarkably independent of the solvent used[40] suggests that the H-substituted substrate is intrinsically more prone to form the *cis* configuration of the double bond, while other substituents shift the preference toward the *trans* product. Understanding these selectivities is of importance for any rational syntheses that strive for maximum yield of the biologically active *trans* product. Both double bonds of the substrate that participate in RCM are located quite far away from the substituent R, so that a direct electronic effect can hardly be envisioned, and the reasons for the observed stereochemistry are unclear.[35] They are investigated computationally in the present paper.

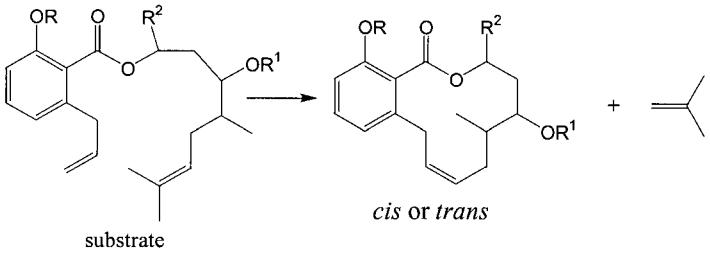

Scheme 3. Ring closure in experimentally studied systems. Refs. [34] and [35]: R = H, Me, MOM, TBS; R^1 = MOM; R^2 = CH_2CH_2OPMB. Ref. [35]: R = H, TBS; R^1 = MOM; R^2 = H (model study).

Model Systems and Computational Methods

Scheme 4 defines the model system chosen for computational study. The H-substituted system **I** (R = H, R′ = H) and the Me-substituted system **II** (R = CH_3, R′ = H) are simplified substrates with a terminal vinyl group. Like the experimentally studied model systems (Scheme 3), substrates **III** (R = H, R′ = CH_3) and **IV** (R = CH_3, R′ = CH_3) carry two additional methyl groups at the terminal double bond. Most of the potential-surface scans employed **I** and **II**, but the most relevant reaction steps were also studied for **III** and **IV**.

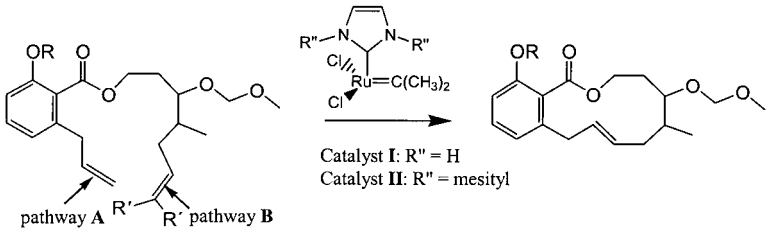

Substrate **I**: R = H, R' = H
Substrate **II**: R = CH_3, R' = H
Substrate **III**: R = H, R' = CH_3
Substrate **IV**: R = CH_3, R' = CH_3

Scheme 4. The computationally studied model systems.

Based on our previous results,[29] we assume a dissociative catalytic mechanism. We used two different catalytic species to assess the influence of substituents at the imidazole ring. Simplified catalyst **I**—dichloro(2-propylidene)(imidazol-2-ylidene)ruthenium—contains an unsubstituted imidazole ring, while catalyst **II** includes two mesityl substituents at this ring, like the real catalyst.[35] The initial reaction steps up to formation of

the second olefin carbene complex (see below) were followed only with catalyst **I**. The subsequent stereo-differentiating steps were investigated for both catalysts.

The quantum-chemical calculations were carried out by using density functional theory (DFT).[41,42] The gradient-corrected BP86 functional was employed, which combines the Becke exchange[43] and Perdew correlation[44] functionals. For ruthenium we used a small-core quasirelativistic effective core potential with the associate (7s6p5d)/[5s3p3d] valence basis set contracted according to a (31111/411/311) scheme.[45] The other elements were represented by the 6-31G(d) basis[46] with one set of d polarization functions at all non-hydrogen atoms. Spherical d functions were used throughout. Thus, the level of theory corresponds to that used in our previous publication.[29]

Geometries were optimized without any constraints. The TURBOMOLE package[47] was employed by taking advantage of the efficient RI-DFT approach.[48] Minima were optimized with a set of $3N-6$ internal coordinates using a default Newton–Raphson-based procedure with BFGS Hessian update, available in TURBOMOLE. Transition states were located by a series of constrained minimizations with subsequent interpolation of the remaining gradient. The procedure was repeated until the gradient vanished within the conventional thresholds of TURBOMOLE (0.001 Hartree $Bohr^{-1}$). The nature of optimized transition states was confirmed by analytic computation of the harmonic force constants employing either TURBOMOLE or Gaussian 03.[49] For transition metal compounds, the chosen DFT approach (BP86 functional with medium-size basis sets) normally provides realistic geometries, relative energies, and vibrational frequencies.[42,50–53] For further validation, in particular for ruthenium systems, we refer to our previous paper.[29]

A fundamental difference between the previously studied parent system[29] and the present RCM system lies in the much larger conformational flexibility of the latter. Energy differences between conformers of the same reactant and product can easily exceed those between *cis* and *trans* isomers. Hence, some systematic approach is needed. We adopted the following strategy. First, the initial olefin carbene complex was optimized by DFT using some reasonable starting conformation of the diene. Then, numerous conformational searches were done using simulated annealing at 2000 K and subsequent cooling to 300 K followed by a regular geometry optimization to generate other conformers. These runs were performed with the Cerius^2 program[54] making use of the UFF force field.[55–57] The catalyst moiety and the olefin double bond along with four neighboring atoms were kept fixed at the DFT geometry. For substrate **I**, artificially high charges were placed at the hydrogen and oxygen atoms to enforce the relevant hydrogen bond (vide infra). For all other atoms, the charges were set to zero. About 20 generated conformers of lowest energy were selected and optimized by DFT. The most stable of these DFT-optimized structures was chosen. This conformation was retained during all steps of the reaction. In reality, of course, a large number of low-energy conformers will be able to react. Our use of just one such low-energy conformer assumes that it is representative for the ensemble of reacting species.

Results

In our choice of model systems (Scheme 4) we have four different substrates **I–IV** and two different catalysts **I** and **II**. Moreover, in the RCM reaction, each of the two double bonds of the diene may coordinate to the catalyst and initiate the reaction, and this gives rise to two different pathways A and B (Scheme 4). Combinatorially, there are thus 16 reaction sequences to be considered, and each pathway will branch at some point to a *cis* or *trans* product.

To limit the computational effort, we performed complete explorations of reaction pathways only for simplified substrates and catalysts. The insights thus gained were used to focus on the relevant reaction steps for the more complex substrates and catalysts. The presentation of results in this section reflects this strategy. Computed energies for the reaction sequences considered are collected in Tables 1–10, while structural drawings are shown in Figures 1–12 and S1–S10 (Supporting Information).

Catalyst I, substrates I and II, path B. *Initiation and first metathesis reaction*: We began the study of the reaction pathway from the product of coordination of the diene substrate **I** to the simplified catalyst **I** (Figure 1). For the sake

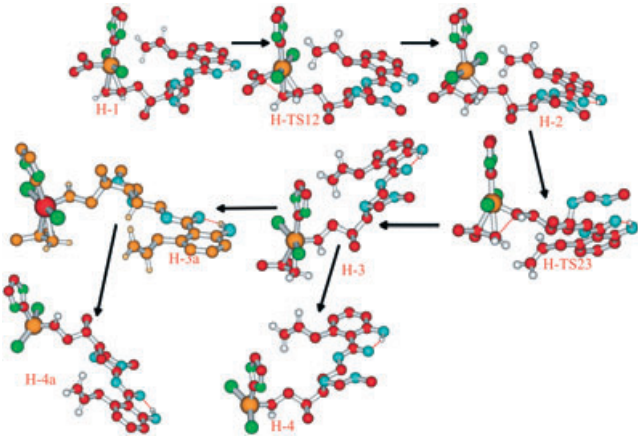

Figure 1. Chain initiation for H-substituted substrate **I**, catalyst **I**, pathway B.

of conciseness, we first consider only pathway B. This olefin carbene complex is labeled in Figure 1 as H-1. This species is qualitatively similar to the olefin carbene intermediate known from the parent system (**II-6** in ref. [29]). An important difference is the orientation of the ligands. The 2-propylidene group in H-1 is no longer perpendicular to the equatorial plane, but partly rotated. Note that conformational preferences in certain carbene complexes were considered earlier.[58–61]

With such orientation of the carbene ligand, the perpendicular conformation of the olefin is no longer preferred. Thus, the olefin double bond is almost parallel to the Ru=$C^{carbene}$ bond. The transformation into metallacycle H-2 proceeds through transition state H-TS12. The metallacycle then rearranges to an isobutene carbene complex H-3, which has a perpendicular conformation of the carbene and isobutene ligands. The barriers for metallacycle formation and breaking are of similar magnitude (about 7 kcal mol^{-1}); the former is slightly higher (Table 1). This differs somewhat from the energy profile of the parent system,[29] where metallacycle cleavage was found to be the rate-determining step, although the difference between the two stages was not very pronounced and the absolute value of the barrier was higher.[29] The final stage of the process is isobutene dissociation, which yields carbene complex H-4. In the parent system this reaction is known to proceed without a transition state.[29] By analogy, the dissociation energy in H-3

Table 1. Chain initiation for substrates **I** (R = H) and **II** (R = Me), catalyst **I** (R″ = H), and pathway B: energies ΔE [kcal mol^{-1}] relative to 1.

Species	H	Me
TS12	7.58	7.64
2	3.45	3.53
TS23	10.38	9.84
ΔE23	6.93	6.31
3	0.07	0.55
3a	0.76	0.57
4	9.30	9.25
4a	7.95	7.87

(about 9 kcal mol^{-1}) is assumed to be the required activation energy. However, this dissociation is unlikely to be rate-determining, since the energetic costs are largely compensated by entropy gain, which is expected to be around 10 kcal mol^{-1} in the gas phase at 298 K.

The carbene complex H-4 has a rotamer with respect to the Ru=C^{carbene} bond (H-4a, Figure 1), which is more stable by 0.5 kcal mol^{-1}. There is a substantial barrier for the conversion between H-4 and H-4a (internal rotation about the Ru=C^{carbene} bond), but their respective precursors, H-3 and H-3a, can be easily transformed into each other. In principle, both H-4 and H-4a can serve as a starting point for subsequent ring closure. In both of these complexes, the carbene ligand is oriented perpendicular to the equatorial plane. Therefore, the stereochemical course of the reaction is not determined at this stage, that is, formation of *cis* and *trans* product is equally possible starting from H-4 or H-4a. The organic chain of the diene substrate does not undergo substantial changes during the entire H-1→H-2→H-3/H3a→H-4/H-4a process, and the hydroxyl and carbonyl groups remain almost coplanar throughout due to hydrogen bonding.

The initiation reactions for the Me-substituted system **II** (see Figure S1 in the Supporting Information) are in general similar to those in the H-substituted system **I**, although there is a noteworthy difference that the methoxyphenyl group in all the complexes **II** is twisted away from the carbonyl group by about 60° (C-C-C-O^{carbonyl} dihedral angle). The energetics resemble those in the H-substituted system **I**.

Ring closure and formation of cis products: Qualitatively, the ring closure part of the RCM reaction involves the same elementary processes as the initiation stage: coordination of the second double bond, metallacycle formation and breaking, and olefin dissociation. However, some of these steps play a different role during ring closure. First, double-bond coordination, which is normally barrier-free and brings an energy gain, is now an intramolecular process and should proceed through a transition state, because the required conformational changes may cost energy. Second, ring formation and cleavage may now be restrained by the presence of the organic chain. All these factors can influence the geometry and energy of the relevant species.

First, we consider the coordination of the free double bond in H-4 (substrate **I**) to the ruthenium atom to give the cyclic olefin carbene complex H-5/H-5a (Figures 2 and 3, Table 2). This species is important, because the position of the carbene ligand may determine the choice of *cis* or *trans* product. However, an almost perpendicular arrangement of the carbene is found, which still allows for the formation of

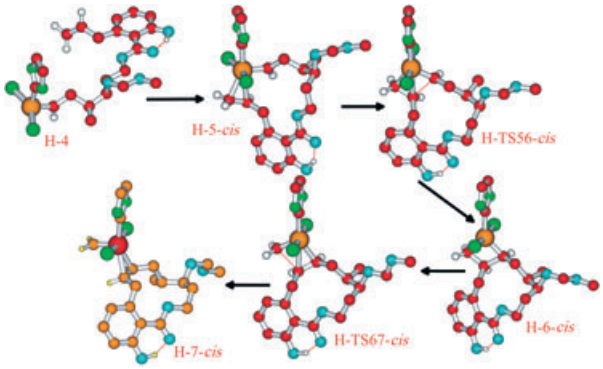

Figure 2. Model catalyst **I**, ring closure for H-substituted system **I** (*cis* pathway).

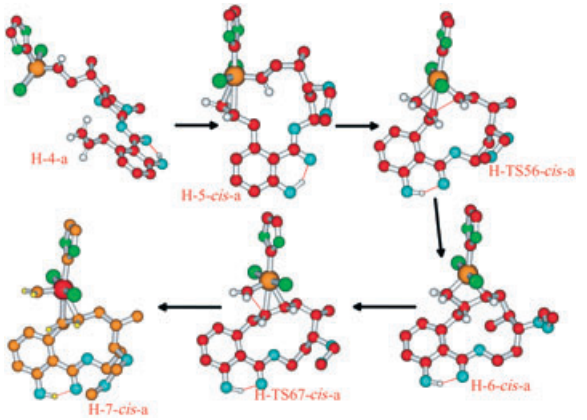

Figure 3. Alternative ring closure for model catalyst **I** and H-substituted system **II** (*cis* pathway).

Table 2. Ring closure for substrates **I** (R = H) and **II** (R = Me), catalyst **I** (R″ = H), and pathway B: energies ΔE [kcal mol^{-1}] relative to 5.

Species	*cis*		*trans*	
	H	Me	H	Me
TS56	5.93	11.58	9.48	7.79
6	2.77	3.69	5.70	3.25
TS67	14.16	8.00	14.15	12.85
ΔE67	11.39	4.31	8.45	9.60
Product	6.39	6.54	4.76	10.98

both *cis* or *trans* product. Therefore, coordination of the second double bond is not decisive for the *cis*/*trans* preference in the simplified system under consideration. Energetically, H-5a is 9.3 kcal mol^{-1} below H-4a, which is equal to the coordination energy of the initial substrate to the catalyst to form H-1. This indicates that even large conformational variations do not lead to any substantial destabiliza-

tion. Clearly, the conversion H-4a→H-5a passes through many small minima and transition states that correspond to conformational changes; it is pointless to look for all of them. We assume that such conformational changes cannot have barriers higher than or comparable to ring closure and cleavage. Entropically, ring closure is unfavorable, with an entropy contribution to ΔG°_{298} that cannot exceed about 10 kcal mol^{-1} at 298 K. Hence, coordination of the second double bond is not the rate-determining step, and the actual *cis*/*trans* discrimination must take place in one of the subsequent reaction steps. Note that the hydrogen bond persists again in all the structures and holds the carbonyl and the hydroxyl groups in one plane.

The formation of the metallacycle occurs through the transition state H-TS56-*cis* with a barrier of 6 kcal mol^{-1}. Metallacycle cleavage (H-6-*cis*→H-TS67-*cis*) must overcome a barrier of 11.4 kcal mol^{-1} and is the rate-determining step in this case.

The reaction of the Me-substituted system **II** (see Figures S2 and S3 in the Supporting Information) proceeds similarly to that of H-substituted system **I** in terms of structure of the reacting species. The methoxyphenyl and carbonyl groups are not coplanar in **II**, as for the chain initiation process. Conversely, the very small barrier for metallacycle cleavage (4.3 kcal mol^{-1}) indicates that metallacycle formation is rate-determining.

Ring closure and formation of trans products: The *trans* products are formed instead of the *cis* ones when the carbene carbon atom in H-5/Me-5 rotates in the opposite direction. In the resulting metallacycle the *cis* or *trans* structure of the product is already determined. Therefore, it is the process 5→TS56→6→TS67→7 that decides the *cis*/*trans* preference.

In the H-substituted system **I** (see Figure S4 in the Supporting Information and Table 2), the entire reaction profile for the *trans* reaction lies higher than that for the *cis* system. The barrier for metallacycle formation is 9.5 kcal mol^{-1}, that is, 3.5 kcal mol^{-1} more than in the *cis* system. The barrier for metallacycle cleavage is 8.5 kcal mol^{-1}, which formally means that metallacycle formation is rate-determining. The difference is very small, however. In the Me-substituted case **II** (see Figure S5 in the Supporting Information), *trans* metallacycle formation and cleavage have barriers of about 7.8 and 9.6 kcal mol^{-1}, respectively.

For comparison of the *cis* and *trans* pathways, we assume that the highest of the two relevant barriers (metallacycle formation and cleavage) are characteristic of the reaction. The *cis*/*trans* barriers are 11.4/9.5 kcal mol^{-1} for substrate **I**, and 11.6/9.6 kcal mol^{-1} for substrate **II**. Therefore, the *trans* isomer should be equally preferred for both systems, despite the dissimilarity of the energy profiles.

We should also consider a different pathway that starts from carbene complex 4-a (Table 3, Figures S6 and S7), in which the organic chain in the carbene is in the *trans* position to the NHC ligand. The energy profile for the reaction 5-a→7-a is rather different from that of the process 5→7. In the case of the *cis* product, metallacycle formation is the rate-determining step. For the *trans* product, the two barriers are comparable. The rate-determining *cis*/*trans* barriers are 10.6/7.8 kcal mol^{-1} for **I** and 12.3/8.1 kcal mol^{-1} for **II**. Hence, the *trans* product is again preferred in both cases, somewhat less so in **I**.

Table 3. Alternative pathway for ring closure for substrates **I** (R = H) and **II** (R = Me), catalyst **I** (R″ = H) and pathway B: energies ΔE [kcal mol^{-1}] relative to 5a.

Species	*cis*		*trans*	
	H	Me	H	Me
TS56-a	8.13	12.31	7.08	10.59
6-a	0.18	3.44	2.24	5.87
TS67-a	3.87	6.95	10.02	15.21
ΔE67	3.69	3.51	7.78	9.33
Product	1.05	4.88	7.91	13.63

Catalyst I*, *substrates I and II*, *path A: ring closure. As shown in Scheme 4, ring-closing metathesis can start from either of the double bonds in the diene substrate and lead to the same final cycloolefin product. All the intermediate stages of the two processes, albeit qualitatively similar, proceed via different intermediates and transition states. This compels us to study both possibilities separately. We only discuss the final part of the reaction for the H-substituted system **I**, that is, ring closure starting from olefin carbene complex H-5 *A* (Figures 4 and S8). There are no large qualitative differences in geometry between the *cis* and *trans* pathways. However, the energetics differ substantially. The energy barriers both for metallacycle formation and breaking are lower for the *cis* process (Table 4). Formally, metallacycle formation is the rate-determining step for the *cis* reaction ($\Delta E^{\neq}$ = 8.5 kcal mol^{-1}), whereas for the *trans* pathway metallacycle cleavage has a slightly higher barrier ($\Delta E^{\neq}$ = 12.2 kcal mol^{-1}). In both cases, the difference between the two stages is small, but the *cis* reaction is clearly preferred (*cis*/*trans* 8.5/12.2 kcal mol^{-1}).

Table 4. Alternative pathway for ring closure for substrates **I** (R = H) and **II** (R = Me), catalyst **I** (R″ = H), and pathway A: energies ΔE [kcal mol^{-1}] relative to 5a.

Species	*cis*		*trans*	
	H	Me	H	Me
TS56-a	8.49	7.03	11.60	7.55
6-a	5.95	5.79	2.64	2.00
TS67-a	13.16	11.38	14.80	11.37
ΔE67-a	7.21	5.59	12.16	9.37
Product	5.38	3.67/3.38[a]	4.80	4.96

[a] Two different conformations.

In the Me-substituted system **II** (see Figures S9 and S10 in the Supporting Information), the *cis* pathway exhibits a higher barrier for metallacycle formation (ca. 7 kcal mol^{-1}), contrary to the H-substituted system **I**. In the *trans* reaction, metallacycle cleavage is rate-determining, with $\Delta E^{\neq}$ =

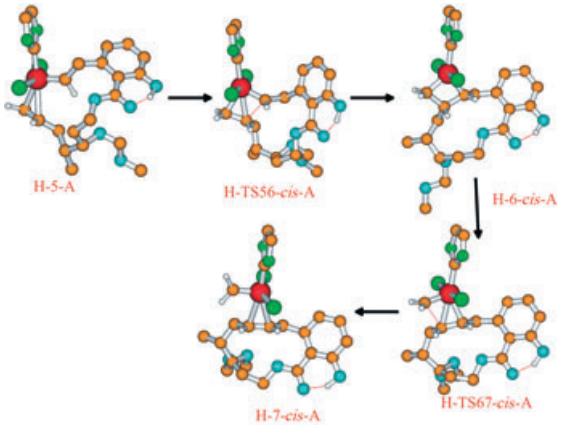

Figure 4. Path A for model catalyst **I**, ring closure for H-substituted system **I** (*cis* pathway).

9.4 kcal mol^{-1}. Thus, to compare the *cis* and *trans* pathways, we need to contrast the *cis*-metallacycle formation barrier (7.0 kcal mol^{-1}) with the *trans*-metallacycle cleavage barrier (9.4 kcal mol^{-1}). Hence, formation of the *cis* product is more favorable by 2.4 kcal mol^{-1}. To sum up, both substrates favor the *cis* product, but the difference to the *trans* product is more pronounced in the case of the H-substituted system (3.7 kcal mol^{-1}).

Catalyst II: general considerations. For catalyst **I**, with an unsubstituted NHC spectator ligand, we have identified the steps in the RCM reaction that can be rate-determining and decide the preference for *cis* or *trans* product. As described above, these are either metallacycle formation or cleavage, depending on the particular case. However, there are no striking differences between *cis* and *trans* pathways that would unambiguously explain the stereochemistry found in the experimental work.[35] The corresponding differences in energy barriers for catalyst **I** are small and cannot be directly transferred to the real catalyst **II**, which has two mesityl substituents on the imidazole ring. Thus, catalyst **II** may display different behavior, mainly because of the steric bulk created by the mesityl groups, which can change the conformational preferences of the organic substrate chain. Mesityl substitution is known[30] to alter the orientation of the NHC ligand with respect to the carbene moiety, such that the plane of the NHC becomes roughly parallel to the M=C^{carbene} bond. In such a situation, one of the mesityl groups will be directed toward the carbene ligand and thus affect the organic chain. This effect should be more pronounced for ring closure and subsequent steps than for the initiation process, because the interaction of the mesityl group with the substituted carbene should be larger than that with the initial 2-propylene ligand.

For a more realistic description, it thus seems mandatory to include the mesityl groups in the computations. This is expensive, however, since the number of basis functions increases to more than 800. The compromise chosen by us was to follow reaction pathways starting from the transition state TS56-R forward to give cycloolefin complex 7-R and backward to give carbene olefin complex 5-R, but ignoring the previous stages of the reaction. In other words, we assume that the structure of TS56-*cis*/*trans*-R can be directly derived from the respective transition state TS56-*cis*/*trans* for the simplified catalyst **I** by replacing the hydrogen atoms in the 2,5-positions of the ligand ring by mesityl groups. The reason for starting from TS56 is that it has a clearly different structure for *cis* and *trans* isomers, while it is not known from the beginning whether 5-R will be analogous to the simplified system or different. The subsequent pathway is then followed as usual by locating the intermediates 5-R and 6-R and transition states TS-56-R and TS-67-R. In the following sections, we present the energetically favored pathways (starting from 5 or 5a).

Catalyst II, substrates I and II, path A: All structures optimized for catalyst **II** (Figures 5–8) share the common characteristic[30] that the NHC plane is parallel to the M=C^{carbene} bond, which significantly affects the steric situation of the organic chain. Apart from the orientation of the ancillary NHC ligand, not much else is changed in H-TS56-*trans*-R-A

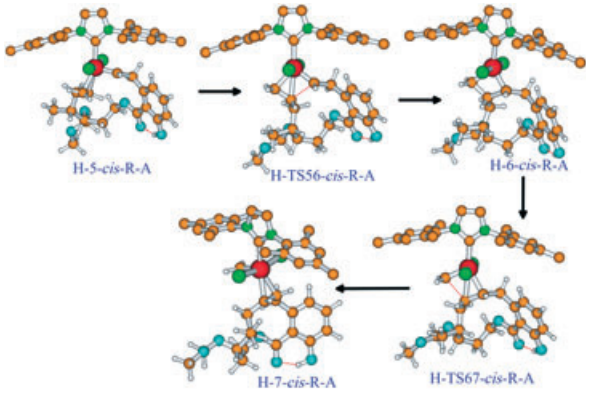

Figure 5. Path A for real catalyst **II** ring closure for H-substituted system **I** (*cis* pathway).

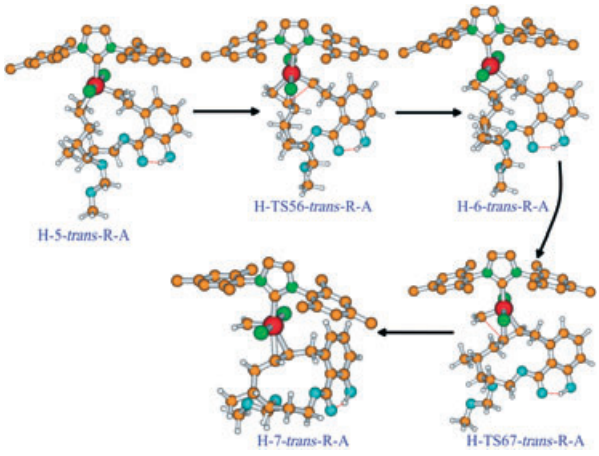

Figure 6. Path A for real catalyst **II**, ring closure for H-substituted system **I** (*trans* pathway).

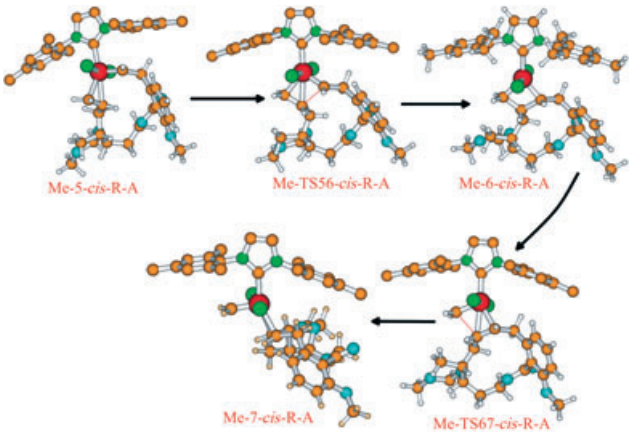

Figure 7. Path A for real catalyst **II**, ring closure for Me-substituted system **II** (*cis* pathway).

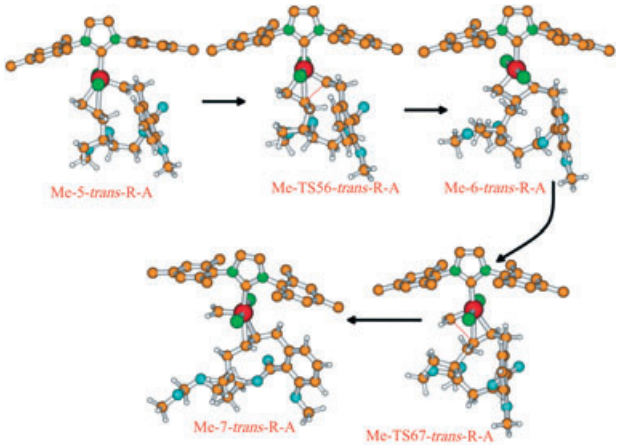

Figure 8. Path A for real catalyst **II**, ring closure for Me-substituted system **II** (*trans* pathway).

compared to H-TS56-*trans*-A (Figure 6). Now, the key question is which transition state leads to this olefin carbene structure. Following the reaction pathway backward starting from H-TS56-*cis*-R-A and H-TS56-*trans*-R-A yields two different olefin carbene structures, H-5-*cis*-R-A and H-5-*trans*-R-A, respectively. The former is more stable by 1.4 kcal mol^{-1}. Both complexes have a clear in-plane orientation of the carbene moiety. This is probably caused not only by the steric bulk of the mesityl groups, but also by the altered electronic situation at the metal center due to reorientation of the π-accepting NHC ligand. The organic chain in the carbene ligand is slightly tilted away from the NHC ligand. Thus, H-5-*cis*-R-A and H-5-*trans*-R-A structurally correspond to H-5a rather than to H-5. H-5-*cis*-R-A and H-5-*trans*-R-A have a perpendicular orientation of the olefin double bond with respect to the Ru=C^{carbene} bond. The transition state for the *cis* pathway, H-TS-67-*cis*-*R*, is a rather early one, with a C···C distance of about 2.2 Å, while that for the *trans* pathway, H-TS-67-*trans*-R, is a late one, with *d*(C···C) ≈ 2.45 Å. This is consistent with the higher energy of H-TS-67-*trans*-R.

The energetics of the reactions for catalyst **II** differ strongly from those of catalyst **I**. The barrier for metallacycle formation is now much lower, while that for metallacycle cleavage is of the same order of magnitude as before. Obviously, this is due to the in-plane orientation of the carbene moiety in catalyst **II** as opposed to a nearly perpendicular orientation in catalyst **I**. Since the position of the carbene ligand in TS56 is always in-plane, a substantial part of the reorganization costs (internal rotation of the carbene ligand) is saved. For the same reason, the relative energy of the metallacycle is much lower for catalyst **II**. Nonetheless, the metallacycle forms a distinct minimum on the potential energy surface. Hence, for catalyst **II**, metallacycle cleavage is the only step of the reaction that can be rate-determining. In contrast, we have seen that either metallacycle formation or cleavage can be rate-determining in the case of the simplified catalyst **I**. Energetic comparison (Table 5) of the *cis* and *trans* pathways favors the *cis* pathway ($\Delta E^{\neq}$ = 6.1 kcal mol^{-1}) over the *trans* pathway ($\Delta E^{\neq}$ = 12.9 kcal mol^{-1}).

Table 5. Ring closure for substrates **I** (R = H) and **II** (R = Me), catalyst **II** (R″ = mesityl), and pathway A: energies ΔE [kcal mol^{-1}] relative to 5-R.

Species	*cis*		*trans*	
	H	Me	H	Me
TS56-R	0.95	1.46	–[a]	2.01
6-R	−3.20	−3.06	−5.6	−3.43
TS67-R	2.93	5.23	7.26	8.04
Δ*E*67-R	6.13	8.29	12.92	11.47
Product	0.39/0.62[b]	3.26	4.4	3.65

[a] The transition state could not be reliably located due to a flat PES, but the barrier is expected to be less than 4 kcal mol^{-1}. [b] Two different conformations.

The Me-substituted substrate **II** is not very different from the H-substituted substrate **I** in the case of the *cis* pathway. The olefin carbene complex has a perpendicular orientation of the olefin double bond and a roughly in-plane position of the carbene moiety. The subsequent reaction steps are analogous to the corresponding stages for substrate **I**. The relative energies are slightly higher for Me-6-*cis*-R-A and H-TS67-*cis*-R-A than for H-6-*cis*-R-A and H-TS67-R-A, respectively. This is probably due to a more flexible chain of the Me-substituted substrate **II**, which allows for better stabilization of the sterically more demanding early reaction stages (TS56-R and 6-R), while this stabilization is less important in Me-TS67-R-A. Consequently, the metallacycle cleavage barrier is just 2.2 kcal mol^{-1} higher than for substrate **I**.

The situation is different in the case of the *trans* pathway (Figures 6 and 8). In Me-5-*trans*-R-A, the olefin double bond is parallel to the Ru=C^{carbene} bond, which is in contrast to the other olefin carbene structures for catalyst **II**. The carbene ligand, however, lies approximately in the in-plane position, though the organic chain is slightly elevated toward the NHC ligand. The parallel position of the double bond in Me-5-*trans*-R-A should be more suitable for forma-

tion of a new bond, and the barrier for metallacycle formation is again rather low (2 kcal mol^{-1}). The relative energy of the metallacycle Me-6-*trans*-R-A is roughly the same as for Me-6-*cis*-R-A, and slightly higher than for H-6-*trans*-R-A. The transition state Me-TS67-*trans*-R-A lies above that for the *cis* reaction. As a consequence, the barrier for metallacycle cleavage is 3.3 kcal mol^{-1} higher on the *trans* pathway than on the *cis* pathway. Hence, the *cis* product is still preferred for the Me-substituted system **II**, but to a lesser extent than in the case of the H-substituted system **I**, since $\Delta\Delta E^{\pm}_{cis-trans}(\mathbf{I}) = 6.8$ kcal mol^{-1}, while $\Delta\Delta E^{\pm}_{cis-trans}(\mathbf{II}) = 3.2$ kcal mol^{-1}.

The product of the reaction, that is, the olefin carbene complex, always has an in-plane arrangement of the carbene ligand relative to the Ru-Cl-Cl plane, and a perpendicular orientation of the olefin double bond with respect to the C=C^{carbene} bond. However, internal rotation of the olefin is essentially free, and several almost degenerate conformers were found in some cases. Energetically, the product olefin complex 7-R lies 3–4 kcal mol^{-1} higher than the isodesmic starting complex 5-R, the difference between the products of various pathways being negligible.

Catalyst II, substrates I and II, path B: As discussed before, the initial coordination of either of the two double bonds of the diene substrate to the catalyst center can lead to the same cycloolefin product. The energetics of these two pathways are rather similar for catalyst **I**, such that neither can be preferred or excluded a priori for catalyst **II**. Thus, the attack of the diene by path B must also be considered. Similarly to path A, we omit the calculation of the initial part of the reaction and focus on the final part starting from the olefin carbene complex 5-R-B (Figures 9 and 10).

First, we describe the *cis* and *trans* pathways for H-substituted substrate **I**. As for the A-side attack, the olefin carbene complexes H-5-*cis*-R-B and H-5-*trans*-R-B (Figures 9 and 10) are already different for the *cis* and *trans* pathways, since they have a roughly in-plane position of the carbene moiety. This would seem to suggest that the stereochemistry

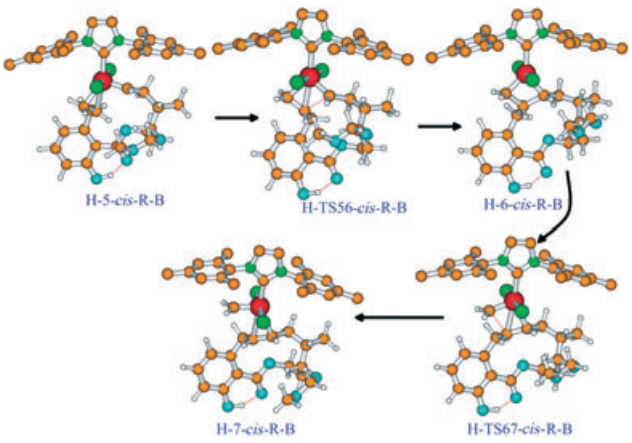

Figure 9. Path B for real catalyst **II**, ring closure for H-substituted system **I** (*cis* pathway).

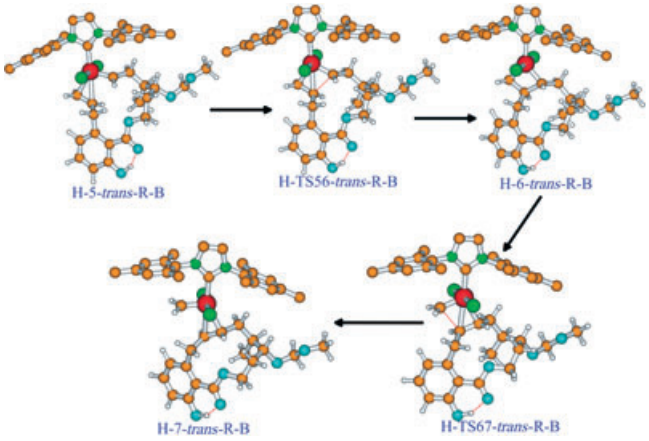

Figure 10. Path B for real catalyst **II**, ring closure for H-substituted system **I** (*trans* pathway).

of the reaction (i.e., whether the *cis* or *trans* product is formed) is already determined at this stage. However, it must be checked whether the two isomers are interconvertible, that is, whether there is a low-barrier process allowing transformation between them. Apparently, such a process will involve internal rotation of the carbene moiety about the Ru=C^{carbene} bond. This rotation can proceed either by moving the organic chain towards the ancillary NHC ligand, or in the opposite direction. The result is expected to be the same, but the respective transition states and barriers will be different. As expected, carbene rotation toward the NHC ligand leads to a considerable repulsion between the carbon chain and the NHC mesityl group and is thus sterically hindered. Indeed, the corresponding barrier is about 9.4 kcal mol^{-1}. Conversely, the opposite rotation is unproblematic and occurs with a barrier as low as 2.5 kcal mol^{-1}. Thus, the difference between H-5-*cis*-R-B and H-5-*trans*-R-B is insignificant for our purposes.

The olefin double bond in H-5-*cis*-R-B is skewed with a dihedral angle C=C-Ru-C^{carbene} of 125°. H-5-*trans*-R-B shows a nearly parallel orientation of the double bond. As expected, the parallel olefin position facilitates metallacycle formation. Thus, the barrier for metallacycle formation is lower for the *trans* pathway (ca. 1 kcal mol^{-1}) than for the *cis* pathway (ca. 2.9 kcal mol^{-1}). The transition state H-TS56-*cis*-R-B has a much shorter C···C distance (2.17 Å) than H-TS56-*trans*-R-B (2.52 Å) (Figures 9 and 10), which indicates a later transition state in the former. Consistent with the Hammond postulate, H-6-*cis*-R-B is less stable than H-6-*trans*-R-B by 4.4 kcal mol^{-1}.

The subsequent transition state for metallacycle cleavage is also lower for the *trans* pathway, by 1.7 kcal mol^{-1}, but the resulting products H-7-*cis*-R-B and H-7-*trans*-R-B are very close in energy. H-7-*cis*-R-B can have both parallel and perpendicular orientation of the olefin double bond with respect to the C=CH$_2$ bond, whereby the parallel conformer is negligibly lower in energy. For H-7-*trans*-R-B, only a parallel structure was found to be a minimum. As a consequence of the above-mentioned energy differences between the *cis* and

trans pathways, the barrier for metallacycle cleavage differs as well: $\Delta E^{\ddagger}_{cis}(\mathrm{H}) = 7.4\ \mathrm{kcal\,mol^{-1}}$, while $\Delta E^{\ddagger}_{trans}(\mathrm{H}) = 10.1\ \mathrm{kcal\,mol^{-1}}$. This indicates a clear preference for the *cis* pathway, although the difference $\Delta\Delta E^{\ddagger}_{cis-trans}(\mathrm{H})$ of $2.7\ \mathrm{kcal\,mol^{-1}}$ should not be prohibitive for the *trans* reaction. To better understand the energy variation along the final part of the reaction pathway, one should take into account the steric hindrance between the mesityl group and the cycloolefin organic chain. Since the angle C^{NHC}-Ru-$C^{carbene}$ increases on passing from 6-R-B to TS67-R-B to 7-R-B, the steric repulsion should decrease. Apparently, the *cis* pathway is more hindered, and the relief is more pronounced. The same effect can be partially responsible for the slightly higher barrier for *cis* metallacycle formation mentioned above. The closeness of the relative energies of the cycloolefin carbene product complexes H-7-R-B can also be accounted for by the higher flexibility of H-7. Since both the cycloolefin ligand and the carbene can rotate relatively freely, there is always room to avoid possible steric repulsion effects. However, the metallacycle and TS67 are largely confined to arrangements imposed by their bonding framework.

We now also consider the final part of the reaction for the Me-substituted substrate **II** with catalyst **II** (Figures 11 and 12). In the case of the initial olefin carbene complex Me-5-*cis*-R-B the parallel orientation of the double bond is preferred (contrary to substrate **I**). As expected, this orientation is well suited for metallacycle formation and leads to a low barrier of $1.5\ \mathrm{kcal\,mol^{-1}}$. More important is the difference in the energy of the metallacycle. Relative to the respective olefin carbene species 5-R-B, Me-6-*cis*-R-B is more stable by $3\ \mathrm{kcal\,mol^{-1}}$ than metallacycle H-6-*cis*-R-B. Apparently, the stabilization due to higher chain flexibility in the compact structure of the metallacycle plays a larger role than in Me-5-*cis*-R-B and in the corresponding transition state Me-TS56-*cis*-R-B. The total effect is that the metallacycle is in a deeper minimum for the Me-substituted substrate **II**. As a result, metallacycle cleavage has a slightly larger barrier (by $1.5\ \mathrm{kcal\,mol^{-1}}$) than for the H-substituted substrate **I**. For the loosely bound cycloolefin carbene product complex, the difference in energy between the two substrates is negligible.

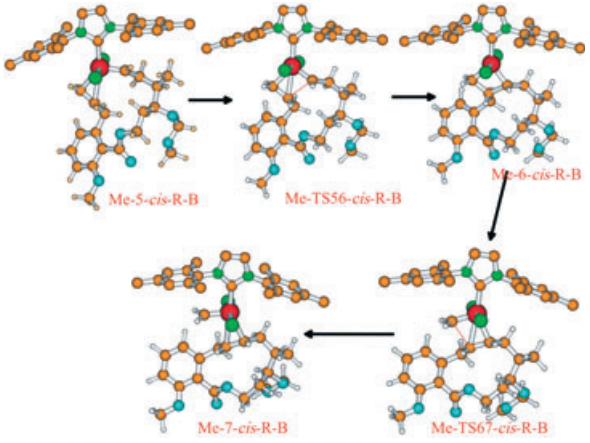

Figure 11. Path B for real catalyst **II**, ring closure for Me-substituted system **II** (*cis* pathway).

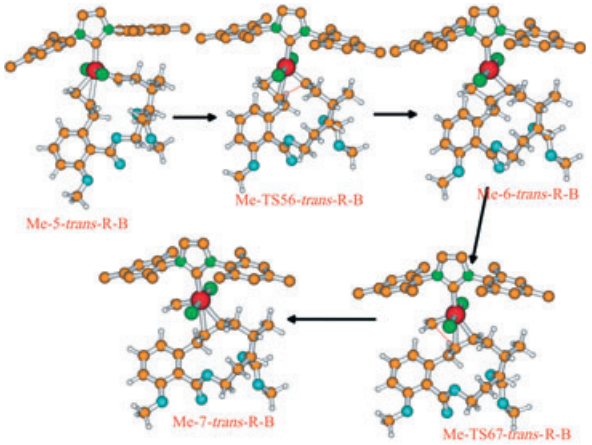

Figure 12. Path B for real catalyst **II**, ring closure for Me-substituted system **II** (*trans* pathway).

For the *trans* pathway the two substrates differ much less. The entire reaction profile is even lower for Me-substituted substrate **II**, but only very slightly. The barrier for metallacycle cleavage is about $0.3\ \mathrm{kcal\,mol^{-1}}$ smaller for Me-substituted substrate **II**, and the resulting cycloolefin carbene product complex has three different conformations, of which the parallel one is still the most stable.

Comparison of the *cis* and *trans* pathways for H-substituted system **I** clearly favors the *cis* product, with $\Delta\Delta E^{\ddagger}_{cis-trans}(\mathrm{H})$ of $2.7\ \mathrm{kcal\,mol^{-1}}$. For the Me-substituted system **II**, the difference between the rate-limiting barriers $\Delta\Delta E^{\ddagger}_{cis-trans}(\mathrm{H})$ is only $0.9\ \mathrm{kcal\,mol^{-1}}$, also in favor of the *cis* reaction.

Catalyst II, substrates I and II, Gibbs free energies: Above, we discussed the potential energy surface (PES) of the ring-closing metathesis in terms of equilibrium electronic energies. The computed relative energies ΔE provide estimates for reaction and activation energies. However, the reaction rate depends on the Gibbs free energy barrier $\Delta G^{\ddagger}$ rather than on $\Delta E^{\ddagger}$. The conversion from $\Delta E^{\ddagger}$ to $\Delta G^{\ddagger}$ includes the zero-point vibrational energy (ZPE) and the temperature-dependent enthalpy and entropy contributions. The typical effect of the ZPE is to decrease energy barriers, while the entropy factor can act in both directions. The computed entropy contributions are dominated by low frequencies, which often suffer from anharmonicity and are quite sensitive to the basis set and method used. Even a small systematic inaccuracy in the frequency evaluation may cause a significant error in the resulting $\Delta S°$ values. Such error sources should be taken into account when considering the $\Delta G°$ values obtained within the harmonic-oscillator/rigid-rotor approximation. In our study of the parent system,[29] we

found that the relative ΔG°_{298} values do not differ strongly from the relative energies ΔE, unless the process in question involves coordination or dissociation.

In our present study of ring-closing metathesis, the coordination of the second double bond to the metal center may also be affected by entropy. For the H-substituted substrate **I** (attack A), the olefin complex is stabilized by about 5.3 kcal mol^{-1} in terms of ΔG°_{298} compared to ΔE, which implies that ring closure can exhibit a substantial $\Delta G^{\neq}$ barrier. Binding the second double bond significantly reduces chain flexibility, and the emerging Ru–C bonds in the olefin carbene complex generally lead to higher harmonic frequencies and thus to decreased entropy and increased zero-point energy (the former effect is more important for ΔG). Even though this causes a substantial change in the barrier ($\Delta G^{\neq}$ versus $\Delta E^{\neq}$), the *cis*/*trans* preference is not affected, because the resulting olefin carbene complex can easily undergo *cis*/*trans* isomerization (vide supra).

The influence of entropy on the later stages of the reaction (except for the dissociation of the resulting cycloolefin) is minor. For the *cis* pathway A in substrate **I** the barrier to metallacycle formation on the ΔG°_{298} surface is just 0.4 kcal mol^{-1} higher than the corresponding ΔE value, while the barrier to metallacycle cleavage is lowered by 0.6 kcal mol^{-1} (see Tables 5 and 6). In the case of *trans* pathway A with substrate **I**, the decrease in the barrier to metallacycle cleavage is larger (about 3.3 kcal mol^{-1}), but the preference for the *cis* pathway is preserved, since $\Delta\Delta G^{\neq}_{cis-trans}$(H) = 3.9 kcal mol^{-1}. For *cis* pathway A with Me-substituted substrate **II**, the same qualitative changes are found, with a decrease in the barrier to metallacycle cleavage of 2.8 kcal mol^{-1}.

Table 6. Ring closure for substrates **I** (R = H) and **II** (R = Me), catalyst **II** (R″ = mesityl), and pathway A: Gibbs free energies ΔG°_{298} [kcal mol^{-1}] relative to 5-R.

Species	*cis*		*trans*	
	H	Me	H	Me
TS56-R	1.34	2.56	–[a]	2.38
6-R	−2.37	−0.5	−2.81/−2.30[b]	−1.71
TS67-R	3.14	4.95	6.78	7.35
$\Delta G^{\neq}_{298}$	5.51	5.45	9.59/9.18	9.06
Product	−1.32	3.39	4.4	2.86/3.56[b]

[a] See footnote a of Table 5. [b] Two different conformations.

In the case of pathway B (see Tables 7 and 8) the transition from ΔE to $\Delta G°$ leads to a slight destabilization of the metallacycle 6-R-B and the transition state TS56-R-B, with a concominant increase in the barrier to metallacycle formation. Since the ZPE contributions tend to decrease barriers, the observed rise is apparently entropically determined and is caused by the new C–C bond emerging in the ring. Consistent with these considerations, the barrier for metallacycle cleavage changes in the opposite way, that is, $\Delta G^{\neq}$ is lower than $\Delta E^{\neq}$ by typically 2–3 kcal mol^{-1}. In spite of these opposite trends in barriers to metallacycle formation and cleavage due to entropy effects, metallacycle breaking remains the stereo-differentiating step in all four cases, and the *cis* pathway remains favored also on the ΔG°_{298} scale, by 3.5 kcal mol^{-1} for substrate **I** and 2.0 kcal mol^{-1} for substrate **II** (see Table 8).

Table 7. Ring closure for substrates **I** (R = H) and **II** (R = Me), catalyst **II** (R″ = mesityl), and pathway B: energies ΔE [kcal mol^{-1}] relative to 5-R-B.

Species	*cis*		*trans*	
	H	Me	H	Me
TS56-R-B	2.88	1.52	0.97	0.63
6-R-B	−1.64	−4.60	−6.06	−6.61
TS67-R-B	5.79	4.32	4.05	3.14
ΔE67-R-B	7.43	8.92	10.11	9.75
Product-par-B	3.13	2.92	3.2	2.18
Product-perp-B	3.27	–	–	4.92/5.17[a]

[a] Two different conformations.

Table 8. Ring closure for substrates **I** (R = H) and **II** (R = Me), catalyst **II** (R″ = mesityl) and pathway B: Gibbs free energies ΔG°_{298} [kcal mol^{-1}] relative to 5-R-B.

Species	*cis*		*trans*	
	H	Me	H	Me
TS56-R-B	4.43	2.57	1.35	3.83
6-R-B	0.33	−1.33	−3.89	−2.55
TS67-R-B	4.91	4.68	4.25	5.45
$\Delta G^{\neq}_{298}$	4.58	6.01	8.09	8.00
product-par-B	1.93	0.93	2.02	3.68
product-perp-B	1.78	–	–	

Catalyst II, substrates III and IV, path A: In the calculations described up to this point, we have neglected two terminal methyl substituents at the double bond in the diene substrate (R′ = H, see Scheme 4) under the tacit assumption that their influence on the reaction kinetics is minor. In view of the small energy differences between *cis* and *trans* pathways, it seems necessary to examine their role. Since we are most interested in the stereo-differentiating stages, the reaction will differ from the unsubstituted case only for path A, in which the corresponding double bond is involved in ring closure. Thus, we decided to follow path A for the dimethylated substrates **III** and **IV** (see Scheme 4) and catalyst **II**, starting from the olefin carbene complex 5 until formation of the product olefin complex. The structures were obtained by reoptimization of the corresponding species without methyl groups.

The results for ΔE obtained for the dimethyl-substituted substrates **III** and **IV** are presented in Table 9. They differ considerably from those for the unsubstituted cases **I** and **II** (Table 5). Most notably, metallacycle 6 is strongly destabilized. This effect is more pronounced for the Me-substituted system **IV**, in which the metallacycle becomes higher in energy than olefin carbene complex 5. This change is unlikely to be of steric origin, since the newly added methyl groups are more remote from the methyl groups in 6 than in 5. It can be rationalized by noting that the extra methyl groups will afford enhanced π donation of the double bond in the π complex and σ donation in the carbene complex,

Table 9. Ring closure for substrates **III** (R = H, R^1 = Me) and **IV** (R = Me, R^1 = Me), catalyst **II** (R″ = mesityl) and pathway A: energies ΔE [kcal mol^{-1}] relative to 5-R.

Species	*cis*		*trans*	
	H	Me	H	Me
TS56-R-B	3.91	6.41	2.30	5.19
6-R-B	0.01	3.09	−4.09	2.38
TS67-R-B	0.70	3.83	2.36	5.70
ΔE67-R	0.69	0.74	6.45	3.32
product-perp	−3.82	−1.30	−2.40	−1.97

Table 10. Ring closure for substrates **III** (R = H, R^1 = Me) and **IV** (R = Me, R^1 = Me), catalyst **II** (R″ = mesityl) and pathway A: Gibbs free energies ΔG°_{298} [kcal mol^{-1}] relative to 5-R-A.

Species	*cis*		*trans*	
	H	Me	H	Me
TS56-R-A	6.47	6.54	3.52	6.98
6-R-A	2.82	4.19	−0.96	4.28
TS67-R-A	3.12	4.40	3.20	7.20
$\Delta G^{\ddagger}_{298}$	0.20	0.21	4.16	2.92
product-perp	−3.89	−2.25	−1.52	−1.97

which stabilize both 5 and 7 without having much influence on 6. The immediate consequence of this destabilization of the metallacycle is that the transition state TS56 is also elevated over 5, thus increasing the barrier for metallacycle formation, which is no longer negligible. As expected, the nature of the transition state is also altered: in the dimethyl-substituted substrates **III** and **IV** this is a much later transition state, which is manifested in substantially smaller $C^{carbene}\cdots C^{olefin}$ distances (by 0.10–0.15 Å). As seen from Table 9, the magnitude of the barrier to metallacycle formation correlates closely with the relative energy of the metallacycle. The computed barriers are lower for substrate **III** (*cis* 3.9 kcal mol^{-1}, *trans* 2.3 kcal mol^{-1}) than for substrate **IV** (*cis* 6.4 kcal mol^{-1}, *trans* 5.2 kcal mol^{-1}).

The second direct consequence of destabilization of the metallacycle by the terminal methyl groups is the strong decrease in the barrier to metallacycle cleavage. This is consistent with the Hammond postulate, since TS-67 becomes energetically closer to 6, which is now higher in energy than 7. A decrease of 5–8 kcal mol^{-1} is observed in all cases compared with substrates **I** and **II** (see Tables 5 and 9). For the *cis* pathway this results in a negligible metallacycle cleavage barrier, while for the *trans* pathway a significant barrier persists.

To summarize, the PES is influenced by terminal methyl groups in a consistent manner: the barrier to metallacycle formation substantially increases with a simultaneous decrease in the barrier to metallacycle cleavage. Consequently, metallacycle cleavage remains the rate-determining step only for the *trans* pathway in the H-substituted system **III**, whereas metallacycle formation becomes rate-determining in all other cases. When comparing the *cis* and *trans* pathways we find that the *cis* reaction is preferred by 2.4 kcal mol^{-1} (6.45/3.91 kcal mol^{-1}) for substrate **III**, whereas the *trans* process is favored by 1.2 kcal mol^{-1} (6.41/5.19 kcal mol^{-1}) for substrate **IV**.

Turning to the Gibbs free energies $\Delta G°$ (Table 10), the rate-determining steps remain the same as before (Table 9), with changes in the barriers ($\Delta G^{\ddagger}$ vs $\Delta E^{\ddagger}$) that are analogous to those discussed for substrates **I** and **II** (see above; increase for metallacycle formation and decrease for metallacycle cleavage). On the ΔG°_{298} scale, the *trans* reaction becomes more favored by 2.3 kcal mol^{-1} for substrate **III**, with a rate-determining metallacycle cleavage barrier $\Delta G^{\ddagger}_{trans}$ = 4.2 kcal mol^{-1}, whereas the *cis* reaction is slightly preferred for substrate **IV**, with $\Delta G^{\ddagger}_{cis}/\Delta G^{\ddagger}_{trans}$ = 6.5/7.0 kcal mol^{-1} for metallacycle formation.

Note that all calculations for substrates **III** and **IV** here refer to path A (see Scheme 4). The alternative path B is also accessible, but the second RCM stage (ring closure) is in this case the same as for substrates **I** and **II**. Comparison of the corresponding barriers $\Delta E^{\ddagger}$ (see Tables 7 and 9) shows that path A is always favored over path B for substrates **III** and **IV** in the second stereo-differentiating RCM stage. However, when considering the Gibbs free energy barriers $\Delta G^{\ddagger}$ (see Tables 8 and 10), the lowest rate-determining barriers are found on path B for the *cis* product (Table 8) and on path A for the *trans* product (Table 10). For both substrates, the relevant free energy barriers lie within 1 kcal mol^{-1} (*cis*/*trans* = 4.6/4.2 kcal mol^{-1} for **III** and 6.0/7.0 kcal mol^{-1} for **IV**).

Discussion and Conclusions

We have studied ring-closing metathesis by second-generation ruthenium-containing Grubbs catalysts for four substrates related to salicylihalamide (Scheme 4). Either of two diene double bonds can coordinate to the metal center to give rise to two different pathways A and B. The first part of the reaction (from initial diolefin coordination to the carbene intermediate 5) was investigated with a simplified catalyst **I**, which has hydrogen atoms in place of mesityl groups. The subsequent second part, which involves ring closure, formation of the metallacycle, and metallacycle cleavage to form the final cycloolefin complex, was considered both for the simplified catalyst **I** and the real catalyst **II** (with mesityl groups). With catalyst **I**, both metallacycle formation and cleavage can be rate-determining steps, and the final stereochemistry results from a complicated interplay between both: for pathway A, the computations show a preference for the *trans* product, whereas pathway B clearly favors the *cis* product both in the H-substituted substrate **I** and, to a lesser extent, in the Me-substituted substrate **II**.

The main difference between catalysts **I** and **II** is the position of the ancillary NHC ligand, which lies in the Ru-Cl-Cl plane in **I**, but is perpendicular to it in **II**. This substantially changes the conformational preferences in the carbene ligand. For catalyst **I**, the olefin carbene complex exhibits a perpendicular out-of-plane orientation of the carbene

moiety, such that both the *cis* and the *trans* products can still be formed. For catalyst **II**, an in-plane orientation is preferred, with an apparent *cis*/*trans* distinction. However, the *cis* and *trans* olefin carbene complexes can be transformed into each other, so it is only later, at the metallacycle cleavage stage, that the stereochemistry is determined. For catalyst **II**, path A shows a preference for the *cis* product, which is more pronounced for the H-substituted substrate ($\Delta\Delta E^{\neq}_{cis-trans}$(H/Me) = 6.8/3.2 kcal mol^{-1}). For pathway B, the *cis* product is also favored, but to a lesser extent ($\Delta\Delta E^{\neq}_{cis-trans}$(H/Me) = 2.7/0.8 kcal mol^{-1}).

The results for the dimethylated substrates **III** and **IV** differ notably from those for the substrates **I** and **II** without terminal methyl groups (catalyst **II**, path B). The main effect of the extra methyl groups is destabilization of the metallacycle, which changes the relative importance of the metallacycle formation and cleavage steps. In this case, the former turns out to be the rate-determining step, while metallacycle cleavage generally becomes a low-barrier process, except for the *trans* product of substrate **III**. On the basis of the computed $\Delta E^{\neq}$ barriers, the *cis* reaction is preferred for substrate **III** ($\Delta\Delta E^{\neq}_{cis-trans} = -2.5$ kcal mol^{-1}), while the *trans* product is slightly favored for substrate **IV** ($\Delta\Delta E^{\neq}_{cis-trans} =$ 1.3 kcal mol^{-1}).

Taking into account ZPE and entropy effects, that is, considering Gibbs free energies ΔG^{o}_{298} rather than energies ΔE, strongly affects the results for coordination and dissociation reactions (steps 1, 4, and 8 in Scheme 2). Moreover, ring closure (coordination of the second double bond, step 5 in Scheme 2) gains a substantial free energy barrier due to a marked entropy loss. However, the stereochemistry of the products is not determined in any of these steps, but rather during either metallacycle formation or cleavage (steps 6 and 7 in Scheme 2), which are influenced less strongly by ZPE and entropy effects: the barriers for metallacycle formation are increased slightly (typically by 0–2 kcal mol^{-1}), while those for metallacycle cleavage are lowered somewhat more (typically by 1–3 kcal mol^{-1}). These shifts do not affect the qualitative conclusions on *cis*/*trans* preference for substrates **I** and **II**, but they modify the qualitative picture for substrates **III** and **IV**, for which the rate-limiting $\Delta G^{\neq}$ barriers for the *cis* and *trans* products now lie within 1 kcal mol^{-1} in each case.

Before attempting a comparison with the available experimental data on stereochemical preferences,[34,35] one should first remember possible limitations of our theoretical approach:

1) The chosen substrates (Scheme 4) are closely related to the experimentally studied systems (Scheme 3), but are generally not identical, except for substrate **III** (= **25** in ref. [35])
2) The chosen catalyst **II** differs from the experimentally employed catalyst[34,35] in the equatorial carbene ligand (2-propylidene instead of benzylidene), but this should be of no concern if the RCM reaction proceeds by a dissociative mechanism with stereo-differentiation in the second part (Scheme 2). In this case, catalyst **II** will represent the catalytically active species.[34,35]
3) The chosen model system does not include solvent or any environmental effects. The experiments[34,35] are carried out in toluene at 80 °C.
4) All DFT calculations refer to a single low-energy conformation of the model system (see Computational Methods), whereas a large number of low-energy conformations are sampled in the experiment.
5) The intrinsic accuracy of DFT calculations is limited.[29,42,50–53]
6) Finally, when converting from ΔE to ΔG^{o}_{298}, the necessary corrections are evaluated in the harmonic-oscillator/rigid-rotor approximation, which is known to be problematic for low-energy vibrations. In the chosen model systems, there are typically around 25 vibrations under 100 cm^{-1}, which strongly contribute to the vibrational entropy and may cause some numerical uncertainty in the computed ΔG^{o}_{298} values.

Given all these caveats, it is clear that quantitative agreement between theory and experiment cannot be expected. In view of the significant differences in the computational results for catalysts **I** and **II**, it is also obvious that one should attempt a comparison with experiment only for the realistic catalyst **II** (with mesityl groups). Here, the computed DFT barriers $\Delta E^{\neq}$ favor the *cis* product for substrates **I** and **III** with R = H (see Scheme 4), in qualitative accord with experiment,[34,35] while they do not give uniform predictions for substrates **II** and **IV** with R = Me (slight preference for *cis* and *trans*, respectively). Substrates **III** and **IV** are closest to the experimentally studied systems[35] labeled **25b** (*cis*/*trans* = 100/0) and **36c** (*cis*/*trans* = 34/66); the quoted observed product distributions are consistent with the relevant DFT barriers $\Delta E^{\neq}$ for **III** (*cis*/*trans* = 3.9/6.5 kcal mol^{-1}) and **IV** (*cis*/*trans* = 6.4/5.2 kcal mol^{-1}). This should be considered as partly fortuitous, however, because the clear *cis*/*trans* distinction for substrates **III** and **IV** is lost on the ΔG^{o}_{298} scale, where the relevant free energy barriers now lie within 1 kcal mol^{-1} (vide supra).

Is it possible to rationalize these computational results a posteriori in a qualitative manner? Two factors appear to be of prime importance, namely, the relative stability of the metallacycle in the second part of the RCM reaction and the flexibility of the chain in the substrate. When going from the model catalyst **I** to the real catalyst **II**, the steric constraints imposed by the two additional mesityl groups favor the compact metallacycle structure; hence, for substrates **I** and **II**, the metallacycle is formed easily with catalyst **II**, such that its cleavage becomes rate-determining for all pathways. The *trans* metallacycle is generally more stable than the *cis* metallacycle (see Tables 5 and 7), and this contributes to smaller *cis* cleavage barriers and consequently to a general preference for the *cis* product. The *cis*/*trans* distinction is more pronounced for substrate **I** (R = H) than for substrate **II** (R = Me) because the former is conformationally more restrained by the O–H···O hydrogen bond in the

chain (see Scheme 4). This hydrogen bond is preserved in substrate **I** on all pathways (see Figures 5, 6, 9, and 10), while the absence of such a restraining factor enables substrate **II** to relax the sterically less favorable *cis* structures (see Figures 7, 8, 11, and 12), such that their energies approach those of the *trans* structures (see Tables 5 and 7). The greater flexibility of the chain in substrate **II** thus leads to a smaller *cis* preference. When going from substrates **I**/**II** to **III**/**IV**, the addition of two terminal methyl groups at one of the double bonds (see Scheme 4) makes the situation even more complex: the second part of the RCM reaction remains unaltered for path B, but changes drastically for path A, since the added methyl groups destabilize the metallacycle significantly through electronic effects (see above) and thus reduce the cleavage barriers significantly (see Table 9). As a consequence, path A is generally favored over path B for substrates **III** and **IV**, and the barriers for metallacycle formation and cleavage become closer to each other. Substrate **III** (R = H) has a more stable *trans* metallacycle and therefore shows a *cis* preference, like substrate **I** (see above), whereas substrate **IV** (R = Me) has similar *cis* and *trans* barriers, like substrate **II**, but with a slight *trans* preference (see Table 9). These considerations indicate that the computational results obtained can indeed be explained in terms of qualitative concepts such as the flexibility of the substrate (presence or absence of hydrogen bonds) and the stability of the metallacycle intermediate (influenced by steric constraints from the catalyst or electronic effects of terminal methyl groups). However, in view of the mechanistic complexity, these rationalizations are only a posteriori and not predictive in a qualitative sense.

In more general terms, the present DFT study illustrates the difficulties of correctly treating subtle stereochemical issues in ring-closing metathesis. It has been established that the *cis*/*trans* stereochemistry of the cycloolefin product is determined in the second part of the RCM reaction, either during metallacycle formation or cleavage. The precise course of events depends on the chosen catalyst and substrate, and both of the a priori possible pathways must be considered. Subtle changes in any of these factors can influence the stereochemical outcome of the RCM reaction through relatively small shifts in the relevant barriers (ΔE^{+}, ΔG^{+}), even though the overall reaction mechanism remains unaltered (Scheme 2).

Acknowledgements

We are grateful to Prof. A. Fürstner for attracting our attention to this field. We thank him, as well as Prof. P. Chen, Dr. C. Adlhart, and Dr. K. Angermund for valuable discussions.

[1] K. J. Ivin, J. C. Mol, *Olefin Metathesis and Metathesis Polymerization*, Academic Press, San Diego, **1997**.
[2] F. Zaragoza Dörwald, *Metal Carbenes in Organic Synthesis*, Wiley-VCH, Weinheim, **1999**.
[3] A. Fürstner, *Angew. Chem.* **2000**, *112*, 3140–3172; *Angew. Chem. Int. Ed.* **2000**, *39*, 3012–3043.
[4] T. M. Trnka, R. H. Grubbs, *Acc. Chem. Res.* **2001**, *34*, 18–29.
[5] a) J. Feldman, R. R. Schrock, *Prog. Inorg. Chem.* **1991**, *39*, 1–74; b) R. R. Schrock, *Tetrahedron* **1999**, *55*, 8141–8153.
[6] S. T. Nguyen, L. K. Johnson, R. H. Grubbs, J. W. Ziller, *J. Am. Chem. Soc.* **1992**, *114*, 3974–3975.
[7] P. Schwab, R. H. Grubbs, J. W. Ziller, *J. Am. Chem. Soc.* **1996**, *118*, 100–110.
[8] Reviews on NHC: a) W. A. Herrmann, C. Köcher, *Angew. Chem.* **1997**, *109*, 2256–2282; *Angew. Chem. Int. Ed. Engl.* **1997**, *36*, 2162–2187; b) A. J. Arduengo, *Acc. Chem. Res.* **1999**, *32*, 913–921.
[9] a) M. Scholl, T. M. Trnka, J. P. Morgan, R. H. Grubbs, *Tetrahedron Lett.* **1999**, *40*, 2247–2250; b) M. Scholl, S. Ding, W. C. Lee, R. H. Grubbs, *Org. Lett.* **1999**, *1*, 953–956.
[10] a) J. Huang, E. D. Stevens, S. P. Nolan, J. L. Petersen, *J. Am. Chem. Soc.* **1999**, *121*, 2674–2678; b) J. Huang, H.-J. Schanz, S. P. Nolan, *Organometallics* **1999**, *18*, 5375–5380.
[11] a) T. Weskamp, F. J. Kohl, W. Hieringer, D. Gleich, W. A. Herrmann, *Angew. Chem.* **1999**, *111*, 2573–2576; *Angew. Chem. Int. Ed.* **1999**, *38*, 2416–2419; b) L. Ackermann, A. Fürstner, T. Weskamp, F. J. Kohl, W. A. Herrmann, *Tetrahedron Lett.* **1999**, *40*, 4787–4790; c) T. Weskamp, F. J. Kohl, W. A. Herrmann, *J. Organomet. Chem.* **1999**, *582*, 362–365.
[12] a) S. M. Hansen, F. Rominger, M. Metz, P. Hofmann, *Chem. Eur. J.* **1999**, *5*, 557–566; b) S. M. Hansen, M. A. O. Volland, F. Rominger, F. Eisenträger, P. Hofmann, *Angew. Chem.* **1999**, *111*, 1360–1364; *Angew. Chem. Int. Ed.* **1999**, *38*, 1273–1276; c) P. Hofmann, M. A. O. Volland, S. M. Hansen, F. Eisenträger, J. H. Gross, K. Stengel, *J. Organomet. Chem.* **2000**, *606*, 88–92.
[13] J.-L. Hérisson, Y. Chauvin, *Makromol. Chem.* **1970**, *141*, 161–176.
[14] E. L. Dias, S. T. Nguyen, R. H. Grubbs, *J. Am. Chem. Soc.* **1997**, *119*, 3887–3897.
[15] M. Ulman, R. H. Grubbs, *Organometallics* **1998**, *17*, 2484–2489.
[16] M. Ulman, R. H. Grubbs, *J. Org. Chem.* **1999**, *64*, 7202–7207.
[17] M. S. Sanford, M. Ulman, R. H. Grubbs, *J. Am. Chem. Soc.* **2001**, *123*, 749–750.
[18] M. S. Sanford, J. A. Love, R. H. Grubbs, *J. Am. Chem. Soc.* **2001**, *123*, 6543–6554.
[19] C. Hinderling, C. Adlhart, P. Chen, *Angew. Chem.* **1998**, *110*, 2831–2835; *Angew. Chem. Int. Ed.* **1998**, *37*, 2685–2689.
[20] C. Adlhart, C. Hinderling, H. Baumann, P. Chen, *J. Am. Chem. Soc.* **2000**, *122*, 8204–8214.
[21] C. Adlhart, M. A. O. Volland, P. Hofmann, P. Chen, *Helv. Chim. Acta* **2000**, *83*, 3306–3311.
[22] M. A. O. Volland, C. Adlhart, C. A. Kiener, P. Chen, P. Hofmann, *Chem. Eur. J.* **2001**, *7*, 4621–4632.
[23] C. Adlhart, P. Chen, *Helv. Chim. Acta* **2003**, *86*, 941–949.
[24] a) O. Eisenstein, R. Hoffmann, A. R. Rossi, *J. Am. Chem. Soc.* **1981**, *103*, 5582–5584; b) A. K. Rappé, T. H. Upton, *Organometallics* **1984**, *3*, 1440–1442; c) T. H. Upton, A. K. Rappé, *J. Am. Chem. Soc.* **1985**, *107*, 1206–1218.
[25] T. R. Cundari, M. S. Gordon, *Organometallics* **1992**, *11*, 55–63.
[26] E. Folga, T. Ziegler, *Organometallics* **1993**, *12*, 325–337.
[27] Y.-D. Wu, Z.-H. Peng, *J. Am. Chem. Soc.* **1997**, *119*, 8043–8049.
[28] a) O. M. Aagaard, R. J. Meier, F. Buda, *J. Am. Chem. Soc.* **1998**, *120*, 7174–7182; b) R. J. Meier, O. M. Aagaard, F. Buda, *J. Mol. Catal. A* **2000**, *160*, 189–197.
[29] S. F. Vyboishchikov, M. Bühl, W. Thiel, *Chem. Eur. J.* **2002**, *8*, 3962–3975.
[30] L. Cavallo, *J. Am. Chem. Soc.* **2002**, *124*, 8965–8973.
[31] C. Adlhart, P. Chen, *J. Am. Chem. Soc.* **2004**, *126*, 3496–3510.
[32] F. Bernardi, A. Bottoni, G. P. Miscione, *Organometallics* **2003**, *22*, 940–947.
[33] C. Costabile, L. Cavallo, *J. Am. Chem. Soc.* **2004**, *126*, 9592–9600.
[34] A. Fürstner, O. R. Thiel, G. Blanda, *Org. Lett.* **2000**, *2*, 3731–3734.
[35] A. Fürstner, T. Dierkes, O. R. Thiel, G. Blanda, *Chem. Eur. J.* **2001**, *7*, 5286–5298.
[36] Y. Wu, X. Liao, R. Wang, X.-S. Xie, J. K. De Brabander, *J. Am. Chem. Soc.* **2002**, *124*, 3245–3253.
[37] A. B. Smith, J. Y. Zheng, *Tetrahedron* **2002**, *58*, 6455–6471.

[38] M. Bauer, M. E. Maier, *Org. Lett.* **2002**, *4*, 2205–2208.
[39] B. B. Snider, F. B. Song, *Org. Lett.* **2001**, *3*, 1817–1820.
[40] A. Fürstner, personal communication, **2001**.
[41] R. G. Parr, W. Yang, *Density Functional Theory of Atoms and Molecules*, Oxford University Press, New York, **1989**.
[42] W. Koch, M. C. Holthausen, *A Chemist's Guide to Density Functional Theory*, Wiley-VCH, Weinheim, **2000**.
[43] A. D. Becke, *Phys. Rev. A* **1988**, *38*, 3098–3100.
[44] J. P. Perdew, *Phys. Rev. B* **1986**, *33*, 8822–8824.
[45] D. Andrae, U. Häussermann, M. Dolg, H. Stoll, *Theor. Chim. Acta* **1990**, *77*, 123–141.
[46] a) W. J. Hehre, R. Ditchfield, J. A. Pople, *J. Chem. Phys.* **1972**, *56*, 2257–2261; b) P. C. Hariharan, J. A. Pople, *Theor. Chim. Acta* **1973**, *28*, 213; c) M. M. Francl, W. J. Pietro, W. J. Hehre, J. S. Binkley, M. S. Gordon, D. J. DeFrees, J. A. Pople, *J. Chem. Phys.* **1982**, *77*, 3654–3665.
[47] a) R. Ahlrichs, M. Bär, M. Häser, H. Horn, C. M. Kölmel, *Chem. Phys. Lett.* **1989**, *162*, 165–169; b) O. Treutler, R. Ahlrichs, *J. Chem. Phys.* **1995**, *102*, 346–354; c) K. Eichkorn, O. Treutler, H. Öhm, M. Häser, R. Ahlrichs, *Chem. Phys. Lett.* **1995**, *242*, 652–660.
[48] K. Eichkorn, O. Treutler, H. Öhm, M. Häser, R. Ahlrichs, *Chem. Phys. Lett.* **1995**, *240*, 283–289.
[49] Gaussian 03, Revision B.01, M. J. Frisch, G. W. Trucks, H. B. Schlegel, G. E. Scuseria, M. A. Robb, J. R. Cheeseman, J. A. Montgomery, Jr., T. Vreven, K. N. Kudin, J. C. Burant, J. M. Millam, S. S. Iyengar, J. Tomasi, V. Barone, B. Mennucci, M. Cossi, G. Scalmani, N. Rega, G. A. Petersson, H. Nakatsuji, M. Hada, M. Ehara, K. Toyota, R. Fukuda, J. Hasegawa, M. Ishida, T. Nakajima, Y. Honda, O. Kitao, H. Nakai, M. Klene, X. Li, J. E. Knox, H. P. Hratchian, J. B. Cross, C. Adamo, J. Jaramillo, R. Gomperts, R. E. Stratmann, O. Yazyev, A. J. Austin, R. Cammi, C. Pomelli, J. W. Ochterski, P. Y. Ayala, K. Morokuma, G. A. Voth, P. Salvador, J. J. Dannenberg, V. G. Zakrzewski, S. Dapprich, A. D. Daniels, M. C. Strain, O. Farkas, D. K. Malick, A. D. Rabuck, K. Raghavachari, J. B. Foresman, J. V. Ortiz, Q. Cui, A. G. Baboul, S. Clifford, J. Cioslowski, B. B. Stefanov, G. Liu, A. Liashenko, P. Piskorz, I. Komaromi, R. L. Martin, D. J. Fox, T. Keith, M. A. Al-Laham, C. Y. Peng, A. Nanayakkara, M. Challacombe, P. M. W. Gill, B. Johnson, W. Chen, M. W. Wong, C. Gonzalez, and J. A. Pople, Gaussian, Inc., Pittsburgh PA, **2003**.
[50] T. Ziegler, *Chem. Rev.* **1991**, *91*, 651–667.
[51] T. Ziegler, *Can. J. Chem.* **1995**, *73*, 743–761.
[52] V. Jonas, W. Thiel, *J. Chem. Phys.* **1995**, *102*, 8474–8484.
[53] See special issue on computational transition metal chemistry: *Chem. Rev.* **2000**, *100*, 351–818.
[54] Cerius^2, MSI Inc., San Diego, CA.
[55] A. K. Rappé, C. J. Casewit, K. S. Colwell, W. A. Goddard III, W. M. Skiff, *J. Am. Chem. Soc.* **1992**, *114*, 10024–10034.
[56] C. J. Casewit, K. S. Colwell, A. K. Rappé, *J. Am. Chem. Soc.* **1992**, *114*, 10035–10046.
[57] A. K. Rappé, K. S. Colwell, C. J. Casewit, *Inorg. Chem.* **1993**, *32*, 3438–3450.
[58] T. E. Taylor, M. B. Hall, *J. Am. Chem. Soc.* **1984**, *106*, 1576–1584.
[59] H. Jacobsen, T. Ziegler, *Organometallics* **1995**, *14*, 224–230.
[60] S. F. Vyboishchikov, G. Frenking, *Chem. Eur. J.* **1998**, *4*, 1428–1438.
[61] M. Cases, G. Frenking, M. Duran, M. Solà, *Organometallics* **2002**, *21*, 4182–4191.

Received: September 29, 2004
Revised: February 2, 2005
Published online: April 19, 2005

